

Distance protection of multiple-circuit shared tower transmission lines with different voltages

Part I: Fault current magnitude

Silva, Filipe Miguel Faria da; Bak, Claus Leth

Published in:
IET Generation, Transmission & Distribution

DOI (link to publication from Publisher):
[10.1049/iet-gtd.2016.1763](https://doi.org/10.1049/iet-gtd.2016.1763)

Creative Commons License
CC BY-NC-ND 4.0

Publication date:
2017

Document Version
Accepted author manuscript, peer reviewed version

[Link to publication from Aalborg University](#)

Citation for published version (APA):
Silva, F. M. F. D., & Bak, C. L. (2017). Distance protection of multiple-circuit shared tower transmission lines with different voltages: Part I: Fault current magnitude. *IET Generation, Transmission & Distribution*, 11(10), 2618-2625. <https://doi.org/10.1049/iet-gtd.2016.1763>

General rights

Copyright and moral rights for the publications made accessible in the public portal are retained by the authors and/or other copyright owners and it is a condition of accessing publications that users recognise and abide by the legal requirements associated with these rights.

- Users may download and print one copy of any publication from the public portal for the purpose of private study or research.
- You may not further distribute the material or use it for any profit-making activity or commercial gain
- You may freely distribute the URL identifying the publication in the public portal -

Take down policy

If you believe that this document breaches copyright please contact us at vbn@aub.aau.dk providing details, and we will remove access to the work immediately and investigate your claim.

Distance protection of multiple-circuit shared tower transmission lines with different voltages. Part I: Fault current magnitude

F. Faria da Silva^{1*}, Claus L. Bak¹

¹ Department of Energy Technology, Aalborg University, Pontoppidanstraede 111, Aalborg, Denmark

* ffs@et.aau.dk

Abstract: Multiple-circuit transmission lines combining different voltage levels in one tower present extra challenges when setting a protection philosophy, as faults between voltage levels are possible. This paper presents a detailed theoretical analysis of such combined faults, including the development of a formula for estimating the magnitude of the short-circuit current. It is demonstrated that if the faulted phase from the higher voltage level leads the faulted phase from the lower voltage level, a distance relay at the higher voltage level sees the fault in the forward direction, whereas a distance relay at the lower voltage level sees the fault in the reverse direction. The opposite happens if the lower voltage level leads the higher voltage level. It is also demonstrated that the magnitude of fault currents of combined faults is normally slightly larger than of equivalent single-phase-to-ground fault at the higher voltage level. Part II will continue the research work and focus in the fault loop impedance RX diagrams.

1. Introduction

The evolution of the European electrical transmission system demands an increasing number of transmission lines and/or their restructuring, in order to enable a high penetration of electricity generated by renewable sources, while maintaining a high security of supply. At the same time, public opinion opposes the construction of new overhead lines and their commissioning is a long process that may extend up to a decade. Consequently, the use of existing corridors is becoming more relevant and the installation of lines of different voltage levels at the same tower more common. The presence of lines at different voltage levels in the same tower possibilities inter-circuit combined faults between different voltage levels, with conductor galloping and ice throw-off being some of the major causes for these faults. The fault loop impedance measured by distance protection relays is different for these types of faults and it becomes a challenge to ensure a fast trip, as a simple relation between fault loop impedance and line parameters no longer exist.

This article has been accepted for publication in a future issue of this journal, but has not been fully edited.

Content may change prior to final publication in an issue of the journal. To cite the paper please use the doi provided on the Digital Library page.

References [1] and [2] analysed combined faults registered in a multiple-circuit 400kV/150kV line in Denmark showing that the fault loop impedance seen by distance relays is not like for a standard fault in a single line and that the faults may be seen in the reverse direction. The references also discuss that a result of the fault impedance being in the reverse direction is that the evaluation of the maximum trip time may become a tedious process, because it is necessary to verify the reactions from distance relays used to protect neighbour lines and cascade tripping.

A detailed analysis of the impedances of combined lines with focus on the zero-sequence mutual coupling for different configurations, the location of the fault and the protection of such lines is done in [3]. The reference focuses on combined lines of equal voltage with at least a common busbar and it analysed the use of pilot schemes (i.e., using telecommunication between the ends of the protected zone) and the correction of the k_0 factors in such lines, together with a discussion on measurements of the zero-sequence current.

The location of fault in combined lines having multiple-circuits of different voltages is also discussed in [4] and an algorithm using only the positive and negative sequence quantities is proposed, eliminating the problems raised by the larger variations in the zero-sequence.

This paper will propose a protection philosophy for combined multiple-circuit lines with shared towers, based on distance relays without using pilot schemes. The presence of single-phase autoreclosure is considered, as the majority of faults are self-healing, but not the choice of the dead time, being assumed that the dead time associated with a single-phase autoreclosure is sufficient for clearing the fault. A full theoretical analysis of combined faults will be made, in order to assure the generalisation of the results, it will be demonstrated in Part II that the settings used for single-phase-to-ground (SPTG) faults can be used for protecting multiple-circuit lines, with some minor changes and without affecting the proper protection against SPTG faults.

The work is divided into two papers with Part I focusing on the development of a formula for estimating the magnitude of the fault current for combined faults, its direction and the respective comparison with SPTG faults at the same location.

Part II focuses on the RX diagrams of the fault loop impedance of combined faults, the comparison with the fault loop impedance of SPTG faults at the same location and the development of guidelines that assure the protection of combined multiple-circuit lines with shared towers.

2. Test System

The simulations performed in this paper for demonstrative purposes are based on a real multiple-circuit 400kV/150kV line in Denmark. Figure 1 shows the single-line diagram of the line, Figure 2 shows the tower layout and the position of the phases in the tower [1]. Reference [1] presents also fault recorded data from a real combined fault in the line.

The distance of the different sections is:

- LAG to MAL: 78.21km of overhead line (OHL)
- LAG to KNA: 20.16km of OHL and 1.1km of cable
- KNA to HAT: 1.23km of cable and 24.21km of OHL
- HAT to MAL: 33.84km of OHL

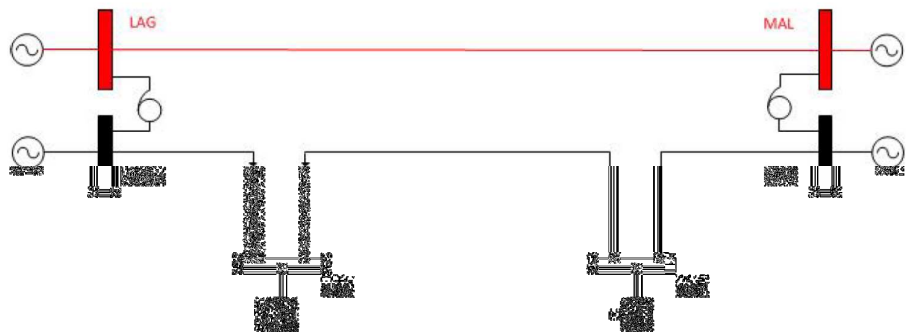


Figure 1 – Single-line diagram of the combined multiple-circuit line. Red: 400kV; Black 150kV. Solid line: OHL; Dashed line: underground cable [1]

This article has been accepted for publication in a future issue of this journal, but has not been fully edited. Content may change prior to final publication in an issue of the journal. To cite the paper please use the doi provided on the Digital Library page.

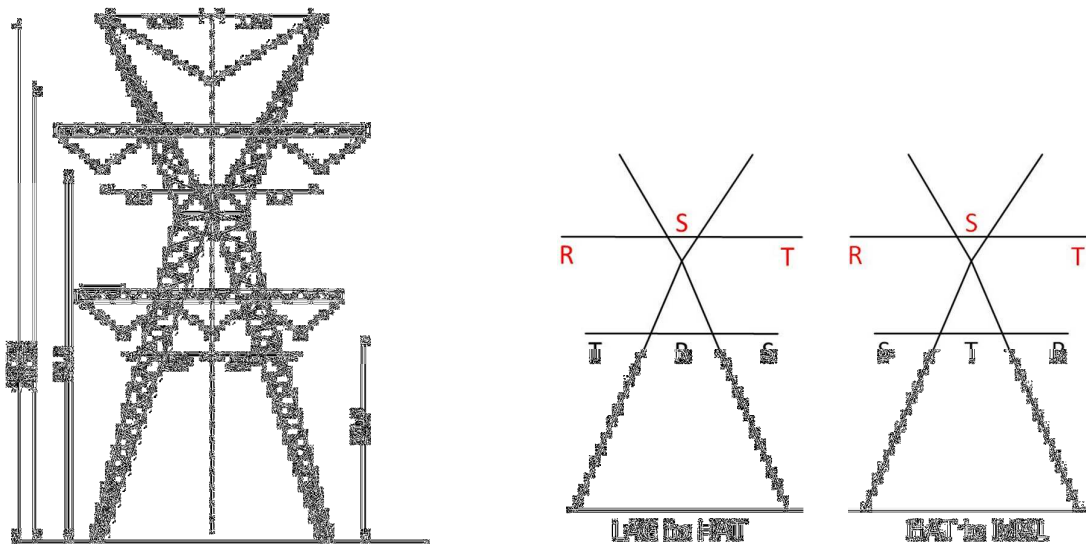


Figure 2 – Left: Double circuit tower: 400kV in delta at the top and 150kV in flat formation at the bottom. Right: Position of the different phases in the tower. Refer to Figure 1 for clarification of LAG, HAT and MAL [1]

3. Analytical expression for the estimation of short-circuit current for combined faults

3.1. Without coupling between phases

The proposal of a protection philosophy using distance protection for combined faults between different voltage levels benefits from an analytical examination of these short-circuits, with the end goal of generalising the results. Figure 3 shows a simplified diagram of a combined 400/150kV circuit for a fault between phases A of the two voltage levels. Typically, there is a transformer connecting the two voltage levels at the substation, not considered here for simplicity, meaning that the coupling between phases at the transformer is also omitted; later simulations for a complete system show that no substantial error is introduced with this simplification, because the transformer's impedance is rather large when compared with the other impedances in the system. The analysis is done first without considering coupling between phases and later extended to include it.

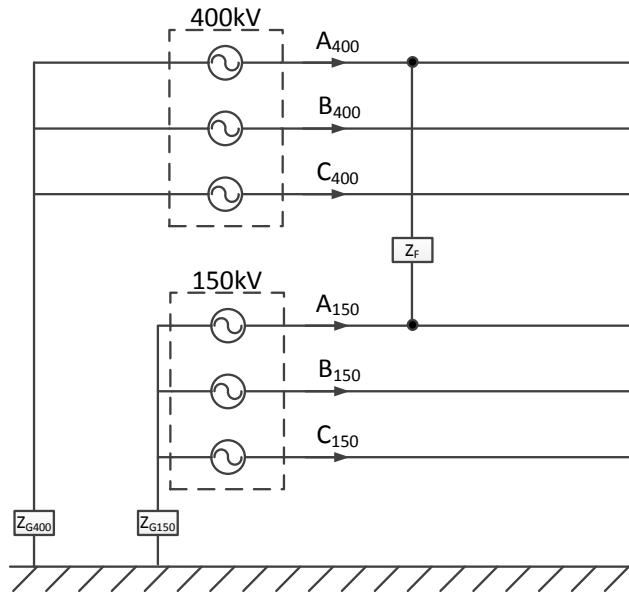


Figure 3 – Single-line diagram for a combined phase-to-phase fault, where Z_F is the fault impedance and Z_{G400} and Z_{G150} are the grounding impedances for the 400kV and 150kV levels respectively

The current in the faulted phases is expected to be much higher than in the sound phases. As a result, the current in the sound phases is considered 0A and neglected, and (1) is written; where $I_{400,x}$ and $I_{150,x}$ are the currents phasors at 400kV and 150kV respectively, and x is the phase.

$$\begin{cases} I_{400,A} = -I_{150,A} \\ I_{400,B} \approx I_{400,C} \approx I_{150,B} \approx I_{150,C} \approx 0 \end{cases} \quad (1)$$

The Fortescue transformation matrix converts the phase currents to symmetrical components (2).

$$\begin{cases} I_{400}^+ = I_{400}^- = I_{400}^0 = \frac{I_{400,A}}{3} \\ I_{150}^+ = I_{150}^- = I_{150}^0 = \frac{I_{150,A}}{3} \end{cases} \quad (2)$$

The voltage difference between the two faulted phases can be written using the fault current and impedances (3). The Fortescue transformation matrix is applied and (3) is rewritten using symmetrical components (4).

This article has been accepted for publication in a future issue of this journal, but has not been fully edited. Content may change prior to final publication in an issue of the journal. To cite the paper please use the doi provided on the Digital Library page.

$$V_{400,A} - V_{150,A} = I_{400,A} (Z_F + Z_{G400} + Z_{G150}) \quad (3)$$

$$(V_{400}^+ + V_{400}^- + V_{400}^0) - (V_{150}^+ + V_{150}^- + V_{150}^0) = 3I_{400}^+ (Z_F + Z_{G400} + Z_{G150}) \quad (4)$$

Equation (4) can be represented by an equivalent symmetrical component circuit, shown in Figure 4.

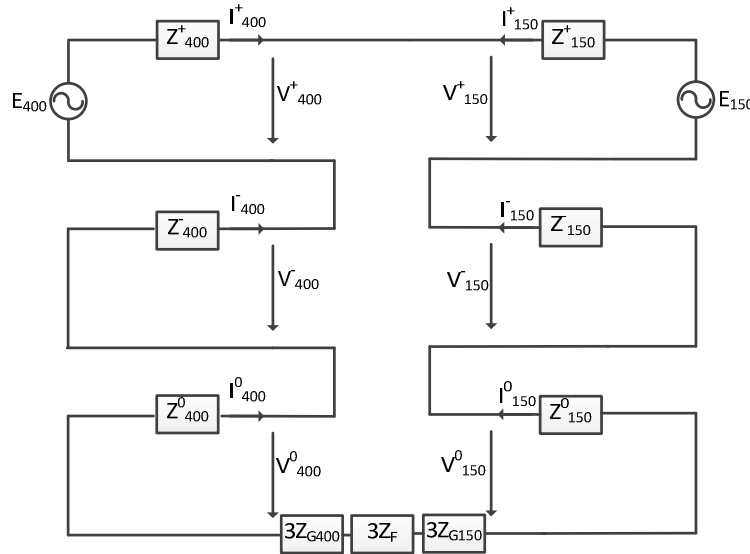


Figure 4 – Equivalent scheme for a combined fault between voltage levels

An expression for estimating the symmetrical currents during combined faults can now be written (5). Table 1 and Table 2 compare the fault current for a fault between the two voltage levels, via simulations in PSCAD/EMTDC and using (5), for a simplified system where a 400kV line is installed in parallel to a 150kV line, both with a length of 100km. The lines' parameters are those of the reference 400kV-150kV system in section 2 and they are modelled using distributed parameters in the simulation. No mutual coupling between the lines of different voltages is present in the simulations, in order to validate the proposed formula in conditions as similar as possible, the next section introduces coupling between voltage levels.

Three cases are considered for a fault at 10km from one of the ends, with case 1 corresponding to a fault between phases A and case 2 to a fault between phase C of the 400kV line and phase A of the 150kV line; in this scenario it is necessary to correct the value of E_{400} or E_{150} in (5) to reflect the phase angle difference. These two cases are subdivided into three sub-cases:

- Case A: Ideal source grounding and solid fault;
- Case B: Ideal source grounding and 2Ω fault impedance;
- Case C: Source grounding impedance of 5Ω and 2Ω fault impedance;

$$\begin{aligned}
 -E_{400} + E_{150} + I_{400}^+ (Z_{400}^+ + Z_{150}^+ + Z_{400}^- + Z_{150}^- + Z_{400}^0 + Z_{150}^0 + 3(Z_F + Z_{G400} + Z_{G150})) &= 0 \\
 \Leftrightarrow I_{400}^+ = I_{400}^- = I_{400}^0 &= \frac{E_{400} - E_{150}}{Z_{400}^+ + Z_{150}^+ + Z_{400}^- + Z_{150}^- + Z_{400}^0 + Z_{150}^0 + 3(Z_F + Z_{G400} + Z_{G150})}
 \end{aligned} \tag{5}$$

The comparison of (5) with the simulations shows that the proposed formula gives values approximate to those of the simulations, even when considering the assumptions made in the formula development. The fault between same phases have a lower current than between different phases, because the numerator of (5) is smaller for the former.

Table 1 – Fault current obtained via simulations and using (5) for the relay closest to the fault

	Case A1	Case A2	Case B1	Case B2	Case C1	Case C2
Calculation [kA]	15.2	31.7	14.4	30.1	8.8	18.2
Simulation [kA]	14.9	31.2	14.1	29.6	8.7	18.2

Table 2 - Fault current obtained via simulations and using (5) for the relay in the far end of the line

	Case A1	Case A2	Case B1	Case B2	Case C1	Case C2
Calculation [kA]	1.7	3.5	1.7	3.5	1.5	3.4
Simulation [kA]	1.6	3.5	1.6	3.3	1.3	2.7

3.2. With coupling between phases

This section extends the formula from the previous section to include mutual coupling between phases. Equation (3) can be extended to consider the voltage drop due to coupling as shown in (6), where $V_{400,M}$ and $V_{150,M}$ are the voltage drops due to inductive coupling in the 400kV and 150kV line, respectively. Capacitive couplings and inductive coupling with sound phases are neglected, as they have a small influence when compared with the inductive coupling between faulted phases.

$$V_{400,A} - V_{150,A} + V_{400,M} + V_{150,M} = I_{400,A} (Z_F + Z_{G400} + Z_{G150}) \tag{6}$$

This article has been accepted for publication in a future issue of this journal, but has not been fully edited.

Content may change prior to final publication in an issue of the journal. To cite the paper please use the doi provided on the Digital Library page.

This approximation considers again that the current in the sound phases is equal to 0A during the fault and that only the current in the faulted phases induces voltages. In these conditions, (6) can be rewritten as (7), where Z_M is the mutual impedance between the two faulted phases. The Fortescue transformation matrix is used and the faulted current is written with symmetrical components, but maintaining the mutual impedance in the phase domain (8).

$$V_{400,A} - V_{150,A} + Z_M I_{400,A} + Z_M I_{400,A} = I_{400,A} (Z_F + Z_{G400} + Z_{G150}) \quad (7)$$

$$I_{400}^+ = I_{400}^- = I_{400}^0 = \frac{E_{400} - E_{150}}{Z_{400}^+ + Z_{150}^+ + Z_{400}^- + Z_{150}^- + Z_{400}^0 + Z_{150}^0 + 3(Z_F + Z_{G400} + Z_{G150}) - 2 \times (3Z_M)} \quad (8)$$

The same three cases from before are reused for validating the new expression considering mutual coupling in the simulation model. Table 3 and Table 4 show the results.

The comparison of the simulations with the proposed equation (8) shows that the latter provides a good approximation for the relay closer to the fault, with an error similar to the cases without coupling, but some inaccuracy for the relay at the far end of the line. This is explained by the distributed nature of the line impedance that is not considered in the equation, which is based on lumped parameters, together with the lower current magnitude, meaning that a smaller absolute error is bigger relatively.

Table 3 - Fault current when considering mutual coupling, obtained via simulations and using (8) for the relay closest to the fault

	Case A1	Case A2	Case B1	Case B2	Case C1	Case C2
Calculation [kA]	21.9	52.3	20.5	48.0	10.1	21.7
Simulation [kA]	21.5	51.1	19.9	46.6	10.0	21.8

Table 4 – Fault current when considering mutual coupling, obtained via simulations and using (8) for the relay in the far end of the line

	Case A1	Case A2	Case B1	Case B2	Case C1	Case C2
Calculation [kA]	1.8	3.7	1.8	3.7	1.7	3.6
Simulation [kA]	2.3	5.7	2.2	5.2	2.1	4.7

4. Fault loop current of combined voltage faults versus single-phase-to-ground fault

4.1. Theoretical analysis and expectations

The previous section presented a formula (8) that can be used to estimate the fault current for combined faults. A conclusion that can be made is that the fault current flows in the forward direction in one of the voltage levels and in the reverse direction in the other voltage level. If the higher voltage is leading the lower voltage level, the current in the higher voltage level flows in the forward direction; if the higher voltage level is lagging the lower voltage level, the current in the lower voltage level flows in the forward direction. Therefore, the distance relays of one of the voltage levels are expected to see the current in the forward direction during a combined fault and it can be hypothesised that either the distance relays in higher or lower voltage levels see the fault as a SPTG fault in the forward direction and react.

Distance protection relays for OHLs will typically autoreclosure after detecting a fault, in order to assess if the fault is permanent or temporary. An extended protection zone (Z_{1B}) is used for autoreclosing and a distance relay sees up to a length equivalent to 120% of the protected line length, instead of the 85%-90% typically used as a 1st zone for permanent trip opening [5]. The autoreclosure can be in all three-phases or just in the faulted phase, depending on the choice of the system operator, with the single-phase autoreclosure requiring a larger dead time, because of the coupling with the sound phases [6]; moreover, as SPTG faults are normally not so severe as three-phase faults, the critical clearing time can be larger for the former and thus, allowing a larger dead time. A combined fault will have mutual coupling between phases even if all three-phases of one of the voltage levels are open, because of the proximity to the other voltage level that remains connected during the fault; as a result, it is advised to increase the dead time even if applying three-phase autoreclosure.

Faults between two voltage levels are expected to be temporary, as they are mostly caused by conductor galloping or ice throw-off. As a result, if the higher voltage level is leading the lower voltage level the distance relays installed at the higher voltage level are expected, in these conditions, to open and clear the fault, if the fault loop impedance is within Z_{1B} . The distance relays installed at the lower voltage level see the fault in the reverse direction and thus, have a longer reaction time and disconnect later. However, the disconnection at both ends of the higher voltage level at the same time is sufficient, because it interrupts the current loop. The opposite happens if the higher voltage level is lagging the lower voltage level and in that case the distance relays at the lower voltage level are the ones interrupting the fault current loop.

However, the fault loop impedance seen by distance relays are influenced by the fault type and short-circuit impedances, and it has to be assured that the measured fault loop impedances of the combined faults are inside of Z_{1B} used for SPTG faults. The theoretical development done next to assess this situation are for the cases where the higher voltage level leads the lower voltage level, or the two are in phase; the cases where the higher voltage level lags the lower voltage level is addressed via simulations in

Part II. For a better overview the faulted currents are compared first and the fault loop impedances in Part II; this approach also allows assessing the effectiveness of overcurrent relays as a backup protection.

The classic expression equivalent to (8) for a SPTG fault is (9) [7]. If the current computed by (9) is smaller than the one from (8) for similar conditions one should expect that the impedance is smaller for a combined voltage fault than for a SPTG fault. In this scenario, the system is protected when using typical protection settings, assuming that the voltage at the busbar is not much affected by the fault, i.e., that the network is strong; later sections of the paper address this issue and the behaviour for weaker networks. Thus, the next step is to compare the two fault currents.

$$I_{400}^+ = I_{400}^- = I_{400}^0 = \frac{E_{400}}{Z_{400}^+ + Z_{400}^- + Z_{400}^0 + 3(Z_F + Z_{G400})} \quad (9)$$

The numerator of (9) can be larger or smaller than the one from (8) depending on the phases involved in the fault and their phase angle difference. As an example and assuming that the two voltage levels are approximately in phase, the numerator for a combined fault (8) is lower than for a SPTG fault (9) if the combined fault is in the same phase for both voltages and higher if it happens between different phases.

The denominator depends on more factors, for example the sequence and grounding impedances from the lowest voltage level increase the value, whereas the mutual coupling decreases it. The positive and zero sequence impedances of a line can be approximated by (10) and (11), respectively; where Z_{AA} , Z_{BB} and Z_{CC} are the self-impedances of phases A, B and C, and Z_{AB} , Z_{AC} and Z_{BC} are the mutual impedances.

$$Z^+ = \frac{1}{3}(Z_{AA} + Z_{BB} + Z_{CC} - Z_{AB} - Z_{AC} - Z_{BC}) \quad (10)$$

$$Z^0 = \frac{1}{3}(Z_{AA} + Z_{BB} + Z_{CC} + 2(Z_{AB} + Z_{AC} + Z_{BC})) \quad (11)$$

The cross-section area of the conductors from the lower voltage level is typically smaller than that of the higher voltage level; as a result, it is expected that the lower voltage level has a higher resistance. The self-reactance of all phases is expected to be similar if no earth wires are present. With earth wires, the self-reactance of the two voltage levels is similar if the phases are symmetrical regarding the vertical axis of the tower, but different if one of the voltage levels has the conductors closer to the earth wires; in this case

the self-reactance of the higher conductors is lower, which corresponds to the higher voltage level, normally. The mutual impedance between phases of the same voltage level, mainly mutual-reactance, is expected to be larger for the lower voltage level, because of the lower distance between phases.

The relation between the self and mutual impedances depends on the distance between phases. The relation between the reactances is approximately given by (12) [8], where, d_{ij} is the distance between phases, GMR is the geometric mean radius of the phase and D_e is given by (13), where ρ is the earth resistivity and f is the frequency. With this relation, one can say that the self-reactance is typically between 1.5-3 times larger than the mutual reactance, depending on the cross-section and distance between phases.

$$\frac{X_{self}}{X_{mutual}} = \frac{\ln\left(\frac{D_e}{GMR}\right)}{\ln\left(\frac{D_e}{d_{ij}}\right)} \quad (12)$$

$$D_e = 658.4 \sqrt{\frac{\rho}{f}} \quad (13)$$

Equations (10) and (11) can be written using the classical Carson formulas. This is shown, after simplifications, in (14) and (15), with all mutual reactances considered equal for simplicity. Where r_i is the conductor AC resistance, r_d is given by (16), X_S is the self-reactance and $X_{M_{SV}}$ is the mutual reactance.

$$Z^+ = \frac{1}{3} \left(3(r_i + r_d) - 3r_d + j3X_S - j3X_{M_{SV}} \right) \quad (14)$$

$$Z^0 = \frac{1}{3} \left(3(r_i + r_d) + 6r_d + j3X_S + j6X_{M_{SV}} \right) \quad (15)$$

$$r_d = 9.869 \times 10^{-7} f \left[\Omega / m \right] \quad (16)$$

Analysing (14) and (15), together with the relation between resistance and reactances previously given, it is expected that the positive-sequence resistance is larger for the lower voltage level, whereas the positive-sequence reactance is larger for the higher voltage level. The zero-sequence resistance should be approximately the same for both voltage levels, as the r_d term is equal for both and it dominates the equation, whereas the zero-sequence reactance is expected to be larger for the lower voltage level; in summary, the relations given in (17) are expected:

This article has been accepted for publication in a future issue of this journal, but has not been fully edited.
Content may change prior to final publication in an issue of the journal. To cite the paper please use the doi provided on the Digital Library page.

$$\begin{cases} R_{400}^{+-} < R_{150}^{+-} \\ R_{400}^0 \approx R_{150}^0 \\ X_{400}^{+-} > X_{150}^{+-} \\ X_{400}^0 < X_{150}^0 \end{cases} \quad (17)$$

Equation (18) shows the subtraction of the denominators of (8) and (9). The impedances can be replaced by resistances and reactances, as given in (19), where the mutual-reactance between the phases of the 150kV level are consider all equal.

$$Z_{CF_Den} - Z_{SPTG_Den} = Z_{150}^+ + Z_{150}^- + Z_{150}^0 + 3(Z_{G150}) - 2 \times (3Z_M) \quad (18)$$

$$\begin{aligned} Z_{CF_Den} - Z_{SPTG_Den} &= 2(r_i + jX_S - jX_{M_SV}) + r_i + 3r_d + jX_S + j2X_M - 6r_d - j6X_M + 3Z_{G150} \Leftrightarrow \\ &\Leftrightarrow Z_{CF_Den} - Z_{SPTG_Den} = 3(r_i - r_d) + j3X_S - j6X_M + 3Z_{G150} \end{aligned} \quad (19)$$

The relation between r_i and r_d depends on the material, cross-section and number of subconductors in a bundled conductor. If only one conductor per phase is used, the two should be similar in magnitude, but r_d is expected to be larger than r_i if bundled conductors are present, assuming that the radius of the conductor(s) is the same. In the first case the resistance is similar for a SPTG fault and for a combined fault, whereas in the second it is larger for a SPTG fault, when not considering the grounding resistance. If the grounding is not solid, the grounding impedance should dominate and the resistance is larger for a combined fault, but this is not expected at transmission level.

The self-reactance is larger than the mutual reactance between different voltage levels. It was previously indicated that the self-reactance is typically between 1.5-3 times larger than the mutual reactance for the same voltage level. The mutual reactance between different voltage levels is expected to be lower than in the same voltage level, as the distance between phases is larger. As a result, the reactance of a combined fault should be larger than for a SPTG fault.

In conclusion the denominator for a combined fault (8) is expected to have a higher value than for a SPTG fault (9).

Having compared the numerators and denominators of the equations used to estimate the current during a combined fault (8) and SPTG fault (9), one can compare the current magnitudes for the two types of faults.

If the phase angle between the faulted phases of the two voltage levels is small, i.e., the fault is for the same phase at the voltage levels, the faulted current is likely larger for a SPTG fault, as the numerator for the combined fault is lower and the denominator larger. In the test case of this paper, the two voltage levels are connected by an autotransformer and so, that would correspond to have a fault between the same phases (e.g., Ph. A-Ph. A). However, the typical layout of the phases in a tower makes such fault very unlikely (see Figure 2); a layout where the phases of the different circuits are not in the same relative positions is expected in multiple-circuit lines, in order to reduce the unbalance of the system, i.e., if both circuits are installed in flat and one has phase A on the left side, the other circuit will not have phase A in the left side. Therefore, the faults are expected to be between different phases and in that case the numerator is approximately 1.2 times bigger for a combined fault than for a SPTG fault, for a tower with 400kV and 150kV lines.

The relation between the denominators is not a fixed value and it will depend on the geometry of the tower. Using typical values, an approximate relation between 1 and 1.4 is obtained when considering infinite short-circuit power networks and demonstrated in appendix A. Thus, the magnitude of the fault current of a combined fault can be bigger or lower than of a SPTG fault, but it is expected to be larger than for the former if the short-circuit power is not infinite (see appendix A).

For the simplified test system used before, the current is simulated for a combined fault and a SPTG fault. Table 5 shows the current for the three cases previously described; Case C3 is alike Case C2, but with an autotransformers at the busbars linking the two voltage levels. It is seen that the currents are similar, confirming the previous analysis. Simulations with non-infinite short-circuit power are done next and the conclusion is alike the one presented for this simplified system.

Table 5 – Fault current for three different cases for combined and SPTG fault

	Case A2	Case B2	Case C2	Case C3
Combined fault [kA]	51.1	46.6	21.8	38.5
SPTG fault [kA]	50.6	43.3	25.7.3	39.1

4.2. Simulations in full system

The demonstration made in the previous section indicates that distance relays installed in the line feeders can potentially protect the systems against a combined fault in a multiple-circuit line using normal setting for single-phase faults with auto-reclosure and extended zone Z_{1B} .

This article has been accepted for publication in a future issue of this journal, but has not been fully edited.

Content may change prior to final publication in an issue of the journal. To cite the paper please use the doi provided on the Digital Library page.

However, the currents of combined and SPTG faults were compared only for simple systems. In order to demonstrate this result in a realistic power system a set of simulations are prepared. The simulated system is the reference system described in section 2. Faults are simulated in three locations: 10km from MAL, 10km from LAG and at 44km from MAL, the latter being a fault between the 400kV level and a section of the 150kV line that it is not connected to MAL or LAG. The fault is solid and the grounding impedance of the equivalent sources generators is 1Ω . The short-circuit powers of all six equivalent networks may have one of three values: 500MVA, 2000MVA and 6000MVA, randomly selected representing a realistic range of variation and modelled via a Thévenin equivalent with X/R of 10. All combinations are tested resulting in a total of 729 simulations.

Figure 5 and Figure 6 show the fault current RMS value seen from MAL and LAG ends respectively, for a combined fault between voltage levels and a SPTG fault at 400kV. The fault is at 10km from MAL and the ratio between the two fault currents is shown. The vertical lines in the figures correspond to a change of the short-circuit power and the MAL end and Table 6 shows the short-circuit powers at MAL in-between the lines. Figure 7 and Figure 8 shows the difference between the fault currents for faults at the other two other locations. Notice that Figure 5 to Figure 8 show the instant when the short-circuit power changes at MAL, but given that the short-circuit power at the other nodes is changing the fault current is not constant for the areas C1-C9.

Table 6 – Short-circuit power in MVA of the 400kV and 150kV networks at the MAL for in-between lines in Figure 5-Figure 8

	C1	C2	C3	C4	C5	C6	C7	C8	C9
400 kV	500	500	500	2000	2000	2000	6000	6000	6000
150 kV	500	2000	6000	500	2000	6000	500	2000	6000

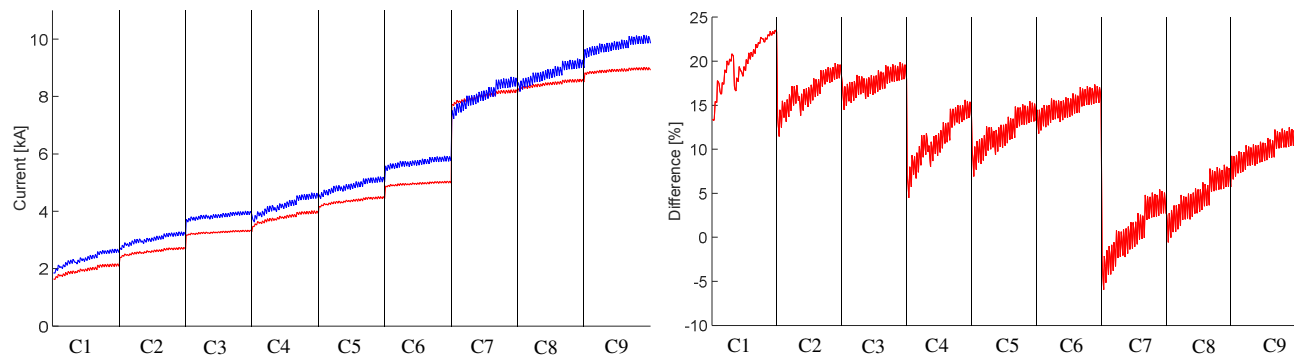


Figure 5 – Left: Fault currents seen from MAL for a combined fault (blue) and a SPTG fault at 400kV (red), both at 10km from MAL; Right: Difference between fault currents with the SPTG fault as reference

This article has been accepted for publication in a future issue of this journal, but has not been fully edited.
Content may change prior to final publication in an issue of the journal. To cite the paper please use the doi provided on the Digital Library page.

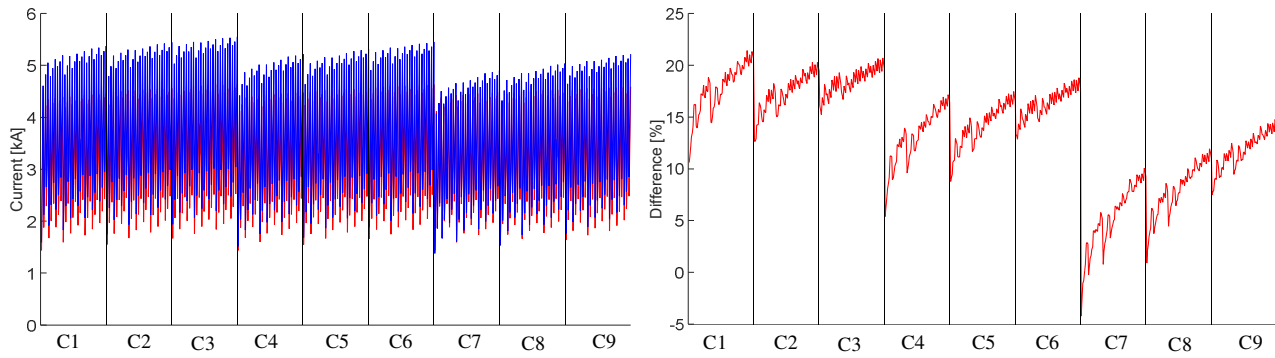


Figure 6 –Left: Fault currents seen from LAG for a combined fault (blue) and a SPTG fault at 400kV (red), both at 10km from MAL; Right: Difference between fault currents with the SPTG fault as reference

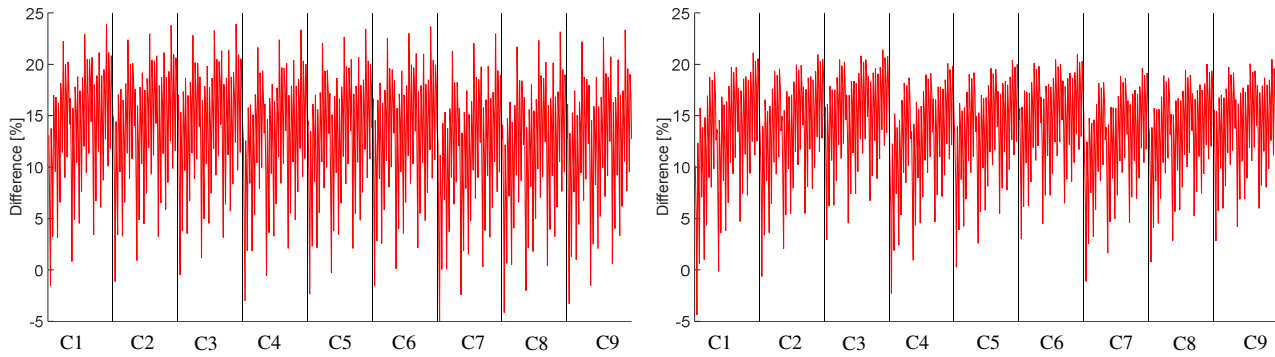


Figure 7 - Difference between fault currents with the SPTG fault as reference, for a fault at 10km from LAG. Left: Seen from LAG; Right: Seen from MAL

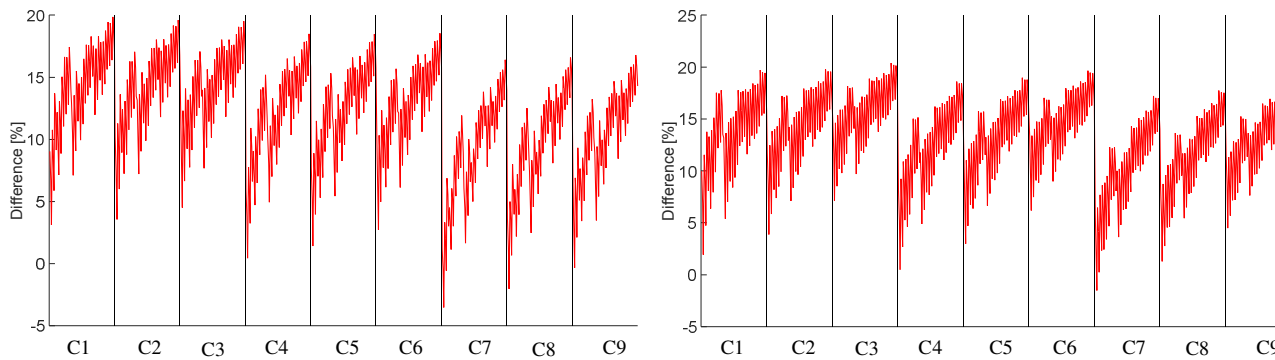


Figure 8 – Difference between fault currents with the SPTG fault as reference, for a fault at 43.84km from MAL. Left: Seen from LAG; Right: Seen from MAL

The simulations confirm the previously results and the fault currents are almost always larger for a combined fault than for a SPTG fault. The exception is only when the 400kV has a large short-circuit

This article has been accepted for publication in a future issue of this journal, but has not been fully edited.

Content may change prior to final publication in an issue of the journal. To cite the paper please use the doi provided on the Digital Library page.

impedance and the 150kV a low one, seen from the end closer to the fault. However, in this case the relation had to be 6000MVA to 500MVA for such to happen and even in that case only when in the presence of low short-circuit powers at the other end of the line.

Therefore, the hypothesis that a combined fault is seen as a SPTG fault and can be cleared is reinforced. However, this cannot be concluded without analysing the phase angles and the impedances, meaning that the RX diagrams should be analysed, which is done in Part II of this paper.

5. Conclusions

This paper is Part I of a two parts paper with the goal of analysing faults between different voltage levels in multiple-circuit transmission lines with shared tower and to present a protection philosophy for such lines, based on distance protection relays without pilot schemes. It was demonstrated that if the higher voltage level leads the lower voltage level, the fault current flows in the forward direction for the former, whereas the latter sees the fault current flowing in the reverse direction; the opposite happens if the higher voltage level lags the lower voltage level. This conclusion was based on an analytical model developed using symmetrical components for combined faults and validated via simulations for different systems and short-circuit powers.

The magnitude of the fault current for combined faults and equivalent SPTG faults was also compared. Equations were developed using typical relations between symmetrical impedances and it was demonstrated that the current magnitude of a combined fault is typically slightly larger than of a SPTG fault at the same location at the higher voltage level; the exception being a system with a high short-circuit impedance in the higher voltage level and low short-circuit impedance in the lower voltage level, but only for a relation of short-circuit powers that is not expected in real systems. This was also confirmed via simulations based in real line.

If overcurrent relays are used as backup protection the comparison of the currents magnitudes demonstrated that they will be able to protect the lines for combined faults. However, the main case of interest is distance relays, without overcurrent relay backup, which requires the analyses of RX diagrams. This analysis is done in Part II of the paper, together with recommendations for the choice of settings of distance relays for the protection of the line in the case of combined faults.

6. References

- [1] Ragnar Sigurbjörnsson, "Combined fault of 400 and 150 kV overhead lines", Master Thesis, Aalborg University, 2015

- [2] C. Leth Bak, R. Sigurbjörnsson, B. S. Bukh, R. Post, “Distance Protection Impedance Measurement for Inhomogeneous Multiple-Circuit 400/150 kV Transmission Lines with Shared Towers”, Development in Power System Protection, DPSP 2016
- [3] Fernando Calero, “Mutual Impedance in Parallel Lines – Protective Relaying and Fault Location Considerations”, 34th Annual Western Protective Relay Conference, 2007, Revised edition, May 2015
- [4] Z. Y. Xu, X. Q. Yan, L. Ran, X. Zhang, “Fault Locating for Inhomogeneous Multiple-Circuit Transmission Lines with Shared Towers”, IEEE-PES General Meeting, 2012
- [5] Alstom Grid, “Network Protection & Automation Guide”, Edition May 2011
- [6] Gerhard Ziegler, “Numerical Distance Protection – Principles and Applications”, Publicis Corporate Publishing, 2nd Edition, 2006
- [7] Nasser Tleis, “Power Systems Modelling and Fault Analysis – Theory and Practice”, Elsevier, 2008
- [8] Arthur R. Bergen, Vijay Vittal, “Power Systems Analysis”, Prentice Hall, 2nd Edition, 2000

7. Appendix A

The relations between the denominators of (8) and (9) is given in (20).

$$\frac{Z_{CF_Den}}{Z_{SPTG_Den}} = \frac{Z_{400}^+ + Z_{150}^+ + Z_{400}^- + Z_{150}^- + Z_{400}^0 + Z_{150}^0 + 3(Z_F + Z_{G400} + Z_{G150}) - 2 \cdot (3Z_M)}{Z_{400}^+ + Z_{400}^- + Z_{400}^0 + 3(Z_F + Z_{G400})} \quad (20)$$

Equation (20) can be written as (21), where a and b are given by (22) and (23), respectively.

$$\frac{Z_{CF_Den}}{Z_{SPTG_Den}} = \frac{a+b}{a} \quad (21)$$

$$a = Z_{400}^+ + Z_{400}^- + Z_{400}^0 + 3(Z_F + Z_{G400}) \quad (22)$$

$$b = Z_{150}^+ + Z_{150}^- + Z_{150}^0 + 3(Z_{G150}) - 2 \cdot (3Z_M) \quad (23)$$

The relation b and a is shown in (24). Simplifications are done and the real parts eliminated, as the reactance is normally dominant, the fault impedance and the grounding impedance are considered 0. With these simplifications (24) is written (25).

$$\frac{b}{a} = \frac{Z_{150}^+ + Z_{150}^- + Z_{150}^0 + 3(Z_{G150}) - 2 \cdot (3Z_M)}{Z_{400}^+ + Z_{400}^- + Z_{400}^0 + 3(Z_F + Z_{G400})} \quad (24)$$

$$\frac{b}{a} = \frac{2X_{150}^+ + X_{150}^0 - 6Z_M}{2X_{400}^+ + X_{400}^0} \quad (25)$$

A thumb rule to compare the zero and positive sequence impedance of overhead lines consists in considering the former 2.5-3 times larger than the latter. One should also remember to include the Thévenin equivalents of the short-circuit powers. Using these relations, (25) is rewritten (26).

This article has been accepted for publication in a future issue of this journal, but has not been fully edited.

Content may change prior to final publication in an issue of the journal. To cite the paper please use the doi provided on the Digital Library page.

$$\frac{b}{a} = \frac{5X_{150}^+ - 6X_M + 3X_{150}^{Th}}{5X_{400}^+ + 3X_{400}^{Th}} \quad (26)$$

A generic relation between X_{400}^+ and X_{150}^+ was given in the main body of the paper, but it was not quantified, because of variability of the parameters. The positive sequence reactance is approximated by (27), as demonstrated in (14). A relation between the self and mutual reactances is given in (30).

$$X^+ = X_S - X_{M-SV} \quad (27)$$

The self-reactances are similar for the two voltage levels and the relation between the mutual can be approximated by (28), where 150 and 400 represent the voltage level.

$$\frac{X_{M-SV}^{150}}{X_{M-SV}^{400}} = \frac{\ln\left(\frac{D_e}{d_{ij}^{150}}\right)}{\ln\left(\frac{D_e}{d_{ij}^{400}}\right)} \quad (28)$$

The distance between phases varies, but one can expect the distance for the 400kV phases to be between 1.25-2.5 times larger than for the 150kV, depending on the configurations used. For typical distances this corresponds in having (28) between 1.05 and 1.25. A value of 1.1 is chosen for this approximation. Consequently, (26) is replaced by (29).

$$\frac{b}{a} = \frac{5.5X_{400}^+ - 6X_M + 3X_{150}^{Th}}{5X_{400}^+ + 3X_{400}^{Th}} \quad (29)$$

The final step is to related the self-impedance with the mutual impedance between voltage levels (30).

$$\frac{X_{400}^+}{X_M} = \frac{\ln\left(\frac{D_e}{GMR}\right) - \ln\left(\frac{D_e}{d_{ij}}\right)}{\ln\left(\frac{D_e}{d_{xy}}\right)} \Leftrightarrow \frac{X_{400}^+}{X_M} = \frac{\ln\left(\frac{d_{ij}}{GMR}\right)}{\ln\left(\frac{D_e}{d_{xy}}\right)} \quad (30)$$

The variable d_{xy} is a vertical distance and it is expected to be between 6m and 12m, whereas d_{ij} is a horizontal distance often between 8 and 15m. A typical value for the GMR is difficult to predict, as the bundling has a strong influence. The ground resistivity may also vary, being often between 50Ωm and 100Ωm in Denmark, but other values can be found in other locations. In these conditions, one finds values

This article has been accepted for publication in a future issue of this journal, but has not been fully edited.

Content may change prior to final publication in an issue of the journal. To cite the paper please use the doi provided on the Digital Library page.

that vary between approximately 1.1 and 1.8, a rather large variation. No indications on typical short-circuit powers can be given, as it is a parameter with a high range.

Using these limits in (21) it is proposed that the relation between the impedance of a combined fault and a SPTG fault is given in (31). The relation is between 1 and 1.4 if one considers the short-circuit power infinite.

$$\frac{Z_{CF_Den}}{Z_{SPTG_Den}} = \frac{a+b}{a} \Leftrightarrow \frac{Z_{CF_Den}}{Z_{SPTG_Den}} = \left[1 + \frac{3X_{150}^{Th}}{5X_{400}^{+} + 3X_{400}^{Th}}; 1 + \frac{2.2X_{400}^{+} + 3X_{150}^{Th}}{5X_{400}^{+} + 3X_{400}^{Th}} \right] \quad (31)$$

The results were validated for a case of two lines of different voltages in parallel all the way, for simplicity. Three different short-circuit powers were considered: 500MVA, 2000MVA and 6000MVA, represented via a Thévenin equivalent with a X/R of 10. Figure 9 shows the results for the 400kV network with 500MVA and 6000MVA using (31) and simulations. The faults were at 10km from one of the ends, for a line 78.21km long. The simulations values vary, because the short-circuit power at the other end is also between 500MVA and 6000MVA. In order to have a better comparison of the results no transformer is considered between the two voltage levels in these simulations.

One can observe that as long as the networks are not too weak, the relation between the faults currents is slightly larger than 1.

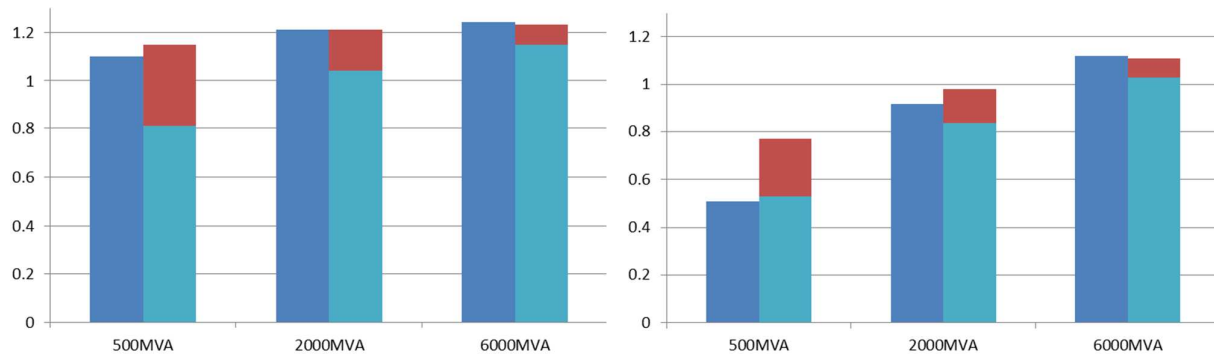


Figure 9 – Relation between combined and SPTG faults for different short-circuit powers from the 150kV network. Left figure: 400kV-500MVA; Right figure: 400kV-6000MVA; Left columns: Equation (31); Right columns: Simulation